New Advanced Operational Regime on the W7-AS Stellarator

K. McCormick,* P. Grigull, R. Burhenn, R. Brakel, H. Ehmler, Y. Feng, F. Gadelmeier, L. Giannone, D. Hildebrandt, M. Hirsch, R. Jaenicke, J. Kisslinger, T. Klinger, S. Klose, J. P. Knauer, R. König, G. Kühner, H. P. Laqua, D. Naujoks, H. Niedermeyer, E. Pasch, N. Ramasubramanian, N. Rust, F. Sardei, F. Wagner, A. Weller, U. Wenzel, and A. Werner

Max-Planck-Institut für Plasmaphysik, EURATOM Association, D-85748 Garching, Germany

(Received 1 February 2002; published 11 June 2002)

A promising new plasma operational regime on the Wendelstein stellarator W7-AS has been discovered. It is extant above a threshold density and characterized by flat density profiles, high energy and low impurity confinement times, and edge-localized radiation. Impurity accumulation is avoided. Quasistationary discharges with line-averaged densities $\bar{n}_e$ to 4×10^{20} m^{-3}, radiation levels to 90%, and partial plasma detachment at the divertor target plates can be simultaneously realized. Energy confinement is up to twice that of a standard scaling. At $B_t = 0.9$ T, an average β value of 3.1% is achieved. The high $\bar{n}_e$ values allow demonstration of electron Bernstein wave heating using linear mode conversion.

DOI: 10.1103/PhysRevLett.89.015001 PACS numbers: 52.55.Hc, 52.55.Rk

The poloidal field divertor is the favored tokamak concept for particle control and mitigation of plasma-wall interaction [1]. This paper reports on advances associated with the first ever realization of the island divertor concept on the Wendelstein stellarator (W7-AS: major radius $R = 2$ m, minor radius $a_{\text{eff}} \leq 0.16$ m, toroidal magnetic field $B_t \leq 2.5$ T), which represents an equivalent solution and is similar in major aspects to that of the Wendelstein 7-X stellarator ($R = 5.5$ m, $a_{\text{eff}} \simeq 0.5$ m), now under construction [2]. In particular, an exciting new confinement regime exhibiting high energy and low impurity confinement has been discovered (here abbreviated IC for "improved confinement"). The IC regime enables attainment of very high densities (up to 4×10^{20} m^{-3}) under controlled, quasistationary conditions—with substantial reduction of power and particle fluxes to material surfaces (partial detachment), an enhancement of the energy confinement time τ_E up to a factor of 2 above τ_E^{ISS95} [3], and a significant reduction of the impurity retention time τ_{imp}. These are essential elements of any confinement concept, potentially making IC the preferred platform for future operation in helical systems.

W7-AS is a modular, low-shear stellarator with five magnetic field periods. Depending on the rotational transform ι_a, the plasma is bounded either by smooth flux surfaces or by a separatrix formed from naturally occurring magnetic islands (at edge iota values $\iota_a = 5/m$ with $m = 8, 9, 10, \ldots$). The five (top-bottom) recently installed divertor module pairs provide an all-graphite plasma-target interaction region (the vessel walls are made of stainless steel) and are optimized for $\iota_a = 5/9$. Control coils act to enhance or reduce the radial extent of the edge islands [4]. On W7-AS in the past, it has been impossible under limiter conditions to produce high-power, high-density, quasistationary neutral beam injection (NBI) discharges with edge densities adequate for acceptable plasma-wall interaction scenarios scalable to a reactor [5,6]. Since τ_E and τ_{particle} as well as τ_{imp} usually increase with density [3,7], such discharges tended to evince impurity accumulation, lack of density control, and subsequent radiation collapse [8].

The IC regime is accessible only via NBI since the transition (line-integrated) density threshold $\bar{n}_e^{\text{thr}}$ lies above the cutoff density ($n_e^{\text{co}} = 1.2 \times 10^{20}$ m^{-3}) for the conventional 140 GHz electron cyclotron resonance (ECRH) heating scheme (second-harmonic X mode). Figure 1 displays characteristic quantities for two discharges, with line-integrated density $\bar{n}_e = 1.5 \times 10^{20}$ m$^{-3} < \bar{n}_e^{\text{thr}}$ (normal confinement, NC) and $\bar{n}_e = 1.63 \times 10^{20}$ m$^{-3} > \bar{n}_e^{\text{thr}}$ (IC), for an absorbed NBI power of $P_{\text{abs}} \simeq 0.7$ MW. For IC, the constancy of total plasma radiation $P_{\text{rad}}(t > 0.32$ s) with time and the higher energy content W is

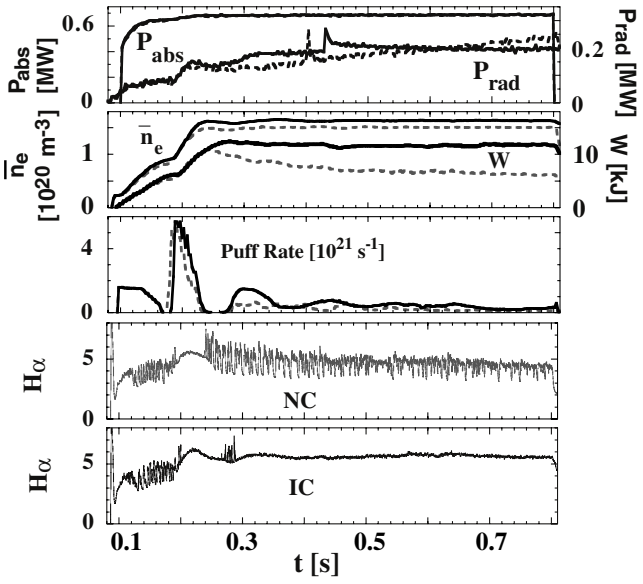

FIG. 1. NC-IC discharges (dashed lines and solid lines, respectively). Time traces of absorbed NBI power P_{abs}, total radiated power P_{rad}, line-averaged density $\bar{n}_e$, plasma energy W, gas puff rate, and the H_α intensity. The spikes in P_{rad} around 0.4 s originate from laser-ablated aluminum.

evident, whereby the faster attainment of stationarity of $W(t)$ in comparison to $P_{\rm rad}(t)$ is typical. The entrance phase into IC is accompanied by H_α bursts at the plasma edge as well as magnetic activity detected by pickup coils (not shown). This, as well as a sheared poloidal plasma flow and associated radial electric field E_r, is characteristic of entrance into an H mode (H^*) free of edge-localized modes (ELMs) on W7-AS [6,9]. The extraordinary difference is the total lack of concomitant peaking of radiation and subsequent radiation collapse, which normally materializes in an H^* phase. A further contrast to H^*, which is accessible within n_e ramps, is that the operational scenario to reliably enter the IC regime requires a rapid density buildup by gas puffing at the very start of the discharge during NBI initiation.

Attendant to IC is a dramatic flattening of the n_e-profile with a sharp gradient at the edge, whereby the separatrix density n_{es} is also considerably augmented. The T_e-profile is enhanced but retains its shape. Figure 2 juxtaposes n_e- and T_e-profiles for NC and IC discharges, for $P_{\rm abs} \simeq 1.4$ MW. Accompanying the NC $\rightarrow$ IC transition is a change in stored energy from $W \simeq 8$–20 kJ, owing to profile changes as well as higher peak values of T_e and n_e (due to higher $\bar{n}_e$). Of major import is the radical change in impurity accumulation as expressed in radiation profiles $P_{\rm rad}(r)$, measured by a bolometer array (Fig. 3): NC is afflicted by peaked $P_{\rm rad}(r)$, whose magnitude increases in time. In contraposition, radiation profiles for IC are peaked at the very plasma edge for moderate densities (attached conditions) and move gradually inwards when partial detachment sets in at higher $\bar{n}_e$ [4]. They remain strikingly stationary with time.

Study of the spatiotemporal behavior of highly ionized states of laser-ablated aluminum provides an indication of impurity transport over the core region (discharges of Fig. 2). The NC regime is characterized by an impurity diffusion coefficient $D \simeq 0.07$–0.1 m^2/s and an inwards convective velocity $v \simeq -10(r/a_{\rm eff})$ m/s. The IC regime yields $D \simeq 0.08$–0.11 m^2/s and $v \simeq -(2$–$3.5) \times (r/a_{\rm eff})$ m/s, i.e., $D({\rm IC}) \simeq D({\rm NC})$, but $v({\rm IC}) < v({\rm NC})$. The NC values for D and v are similar to those found for NBI-heated plasmas previously investigated on W7-AS [10]. They are also comparable to the v/D ratios found on tokamaks in ELM-free H-mode phases [11]. During IC, the reduced inwards pinch evidently causes diffusion to dominate over convection, leading to a reduction of impurity peaking. We note here that earlier studies on W7-AS have shown background ions to display similar confinement behavior to impurities in terms of D [12]. In the present study, the flat n_e-profiles, as well as the realization of density control in IC, are congruous with H^+ transport being related to that of impurities. Definitive statements about transport in the n_e-gradient region are difficult to make: The observation that the density fall-off length $n_e/(dn_e/dr)$ near the separatrix remains constant over the NC $\rightarrow$ IC transition is consistent with an invariant D, in contrast to a transition to H^*.

Figure 4 summarizes the systematic variation of relevant plasma parameters obtained from $\bar{n}_e$-, $P_{\rm NBI}$ scans for quasistationary discharges of duration $\geq$0.5 s. Figure 4(a) shows the energy confinement time $\tau_E = W/P_{\rm abs}$ vs the line-averaged density $\bar{n}_e$. The apparent jumps of τ_E at $\bar{n}_e \simeq (1.5,\ 1.8,$ and $2.1) \times 10^{20}$ m^{-3} (for $P_{\rm NBI} = 1,\ 2,$ and 3.5 MW, respectively) mark the threshold densities $\bar{n}_e^{\rm thr}$ for transition into IC at each power level. τ_E values in NC follow the scaling $\tau_E^{\rm ISS95} = 0.26\iota_a^{0.4} B_t^{0.83} a^{2.21} R^{0.65} \times \bar{n}_e^{0.51} P_{\rm abs}^{-0.59}$ [3], whereas for IC one finds $\tau_E \sim 2 \times \tau_E^{\rm ISS95}$, except during detachment, where $P_{\rm rad}$ profiles begin to encroach into the core plasma (cf. Fig. 3). We note that τ_E is also greater than a dedicated W7-AS scaling [3]. An outstanding feature of IC is that with the increase in τ_E there is a large mitigation in the residence time $\tau_{\rm imp}$ of laser-ablated aluminum [Fig. 4(a)], which at high $\bar{n}_e$

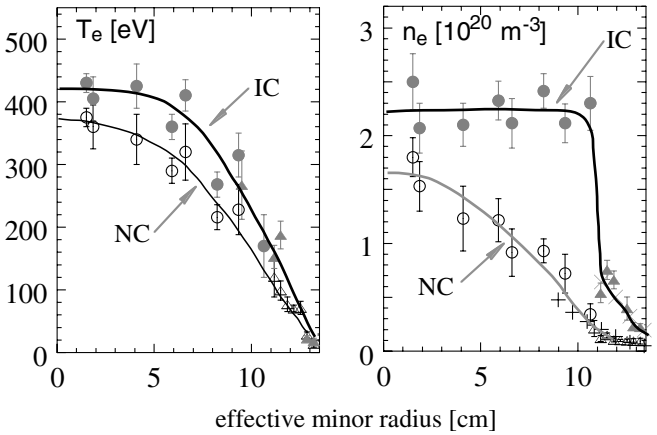

FIG. 2. T_e- and n_e-profiles for normal confinement NC and IC. The separatrix is positioned around $r_{\rm eff} \simeq 12$ cm. Circular points are from the central and triangular points from the edge-Thomson scattering system. n_e values from the lithium-beam system are crossed. The n_e-profile changes are particularly spectacular.

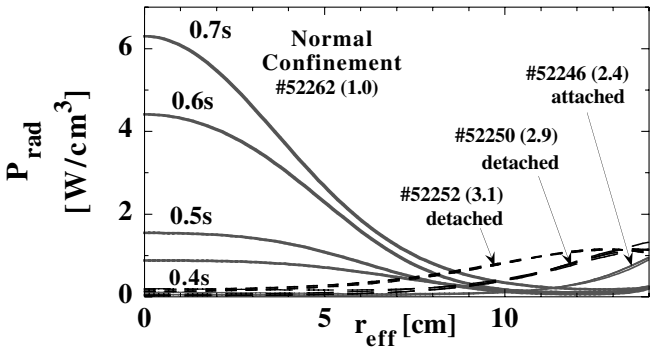

FIG. 3. Radiation profiles from a bolometer array. One NC discharge and three IC discharges are depicted at four time points each over $t = 0.4$–0.7 s. $\bar{n}_e$ (10^{20} m^{-3}) is given in parentheses. Associated $P_{\rm rad}/P_{\rm NBI}$ are NC (0.12–0.3) and IC (0.3, 0.6, and 0.8) in order of increasing $\bar{n}_e$. $P_{\rm NBI} = 2$ MW hydrogen beam injection in H^+ plasma ($H^0 \rightarrow H^+$), $B_t = 2.5$ T, $\delta x = 3.3$ cm.

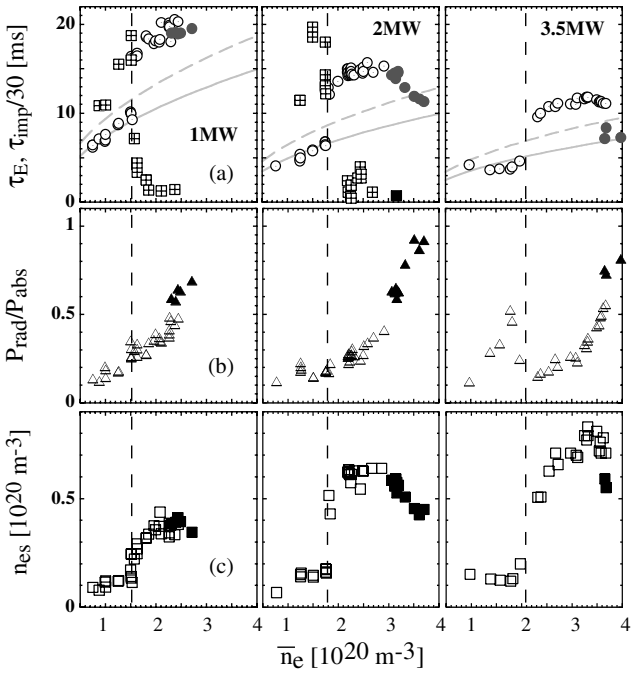

FIG. 4. From left to right for $P_{\mathrm{NBI}} = 1$, 2, and 3.5 MW is shown as follows: (a) τ_E (circles) and τ_{imp} (crossed squares) with τ_E^{ISS95} (solid curve) and τ_E^{W7AS} (dashed curve); (b) radiated power fraction $P_{\mathrm{rad}}/P_{\mathrm{abs}}$; (c) separatrix density n_{es}. Attached plasmas have open symbols, detached are solid. The distance between separatrix and target plates is $\delta x \simeq 3.8$ cm, $B_t = 2.5$ T. The dashed vertical line depicts the NC $\rightarrow$ IC boundary. Note the remarkable increase of τ_E and n_{es} at the transition, in contrast to the decline of τ_{imp}. The influence of IC on P_{rad} is conspicuously evident at 3.5 MW.

approaches that of τ_E. The normalized radiated power $P_{\mathrm{rad}}/P_{\mathrm{abs}}$ shown in Fig. 4(b) grows smoothly with $\bar{n}_e$ until $P_{\mathrm{rad}}/P_{\mathrm{abs}} \simeq 0.5$, when higher values lead to the onset of partial plasma detachment at the target plates. The separatrix density n_{es} [Fig. 4(c)] shows an increase at the NC $\rightarrow$ IC transition point. n_{es} then continues to climb with $\bar{n}_e$, saturates at $n_{es}^{\mathrm{max}} \simeq (4,\ 6,\ \mathrm{and}\ 8) \times 10^{19}$ m^{-3} (for $P_{\mathrm{NBI}} = 1$, 2, and 3.5 MW, respectively) before dropping at partial detachment. τ_E mirrors the general behavior of n_{es}.

Figure 5 shows the peak power flux $P_{\mathrm{tar}}^{\mathrm{peak}}$ and the integral power loading E_{tar} to a target tile (measured by IR thermography and calorimetry) along with the peak H_α (related to particle flux for nondetached cases) vs $\bar{n}_e$ for IC discharges at $P_{\mathrm{NBI}} = 2$ MW. $P_{\mathrm{tar}}^{\mathrm{peak}}$ is reduced by a factor of 10, with a substantial reduction occurring before the onset of detachment. Langmuir probes mounted in the tiles measure densities less than n_{es}, meaning that detachment is obtained without going through the high-recycling regime typical for tokamaks [4]. The 3D edge modeling code EMC3-EIRENE [13,14] generally predicts such trends, i.e., the lack of a high-recycling regime as well as the drop of fluxes to the target plate already at moderate densities. Of note is that these changes are attained on

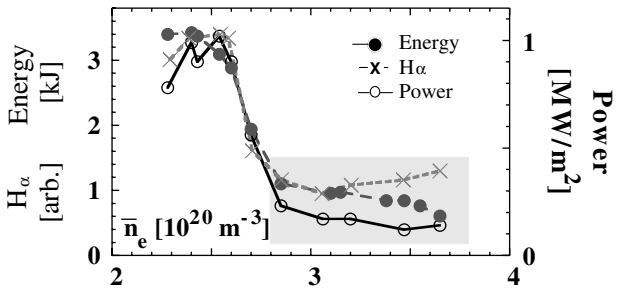

FIG. 5. Energy deposited on a target tile (solid circles), peak H_α intensity (crosses), and peak power flux (open circles) vs $\bar{n}_e$ at $\delta x \simeq 3.3$ cm. $P_{\mathrm{NBI}} = 2$ MW, $\mathrm{H}^0 \rightarrow \mathrm{H}^+$, $B_t = 2.5$ T. Each point represents one stationary discharge. Gray-shaded points are detached.

W7-AS through a combination of increasing n_{es} and P_{rad}. Ultimately, it is the increase in P_{rad} at the edge, leading to a reduction of power flow to the target plates, which drives the discharges into partial detachment. Finally, subdivertor neutral pressures in the 10^{-3} mbar range are attained at high $\bar{n}_e$, predicted to be more than sufficient for effective neutral pumping. Neutral pressures near the wall are typically in the 10^{-4} mbar range for IC.

The results discussed in Fig. 4 are universal in nature with respect to diverted discharges as long as the distance δx between the separatrix and target plates (adjusted via control coils) is greater than 2.4 cm. For $0 \leq \delta x < 2.4$ cm, the IC regime can also be established, albeit with the caveat that at high $\bar{n}_e$ an oscillatory radiation collapse replaces controlled detachment. For high-β studies on W7-AS, the natural islands are compensated by control coils to produce a smooth surface with maximum plasma volume. NBI heating at $P_{\mathrm{NBI}} = 3.5$ MW (with $P_{\mathrm{abs}} = 3$ MW) at $B_t \simeq 0.9$ T, $\iota_a = 0.52$, and $\bar{n}_e = 2.2 \times 10^{20}$ m^{-3} yields a volume-averaged $\langle\beta\rangle = 3.1\%$, with a value of $\simeq 6.4\%$ in the plasma center ($n_e \simeq 2.3 \times 10^{20}$ m^{-3}, $T_i = T_e = 260$ eV). This represents an enhancement in $\langle\beta\rangle$ by 50% over the previous record, whereby here the principal benefits of IC are a reduction in impurity radiation and capability of quasi-steady-state operation. As in former studies [15], no evidence of a β-stability limit is found and only low MHD activity is seen, particularly in the range of maximum β.

For separatrix-bounded plasmas, the path to IC at the beginning of the discharge (and also the backtransition, if present) is often accompanied by H-mode phenomena. In particular, the buildup of an edge-localized transport barrier is evident as well as its intermittent breakdown, manifested in ELMs. IC itself is absolutely ELM-free. The IC regime exhibits similarities with the enhanced D_α H-mode (EDA) found on the Alcator C-Mod tokamak (higher τ_E and higher D_α at the transition, no impurity accumulation) [16]. Also in that case, the transition physics are not yet well understood. However, on W7-AS it is plausible that $\bar{n}_e^{\mathrm{thr}}$ for entrance into IC increases with P_{NBI} as a result of the need to strike a balance between central fueling and

edge density buildup by gas puffing and neutral recycling. Thus, higher P_{NBI} implies higher central fueling, which must be counteracted by higher gas puff rates, resulting in a higher $\bar{n}_e^{\mathrm{thr}}$.

Looking to future steady-state heating scenarios, standard ECRH at 140 GHz cannot support $n_e > 1.2 \times 10^{20}$ m^{-3}. Now, with the ability to sustain discharges in W7-AS at densities in excess of 2.4×10^{20} m^{-3}, it has become feasible to test the efficacy of electron Bernstein wave (EBW) heating, accessible through mode conversion from an O wave to an X wave and then to an EBW (OXB) [17]. Local resonant EBW heating with good power coupling efficiency, comparable with NBI heating, has been demonstrated [4]. 1 MW of NBI heating (out of 2.5 MW) has been successfully substituted using EBW (1.1 MW in optimal polarization for OXB-mode conversion), while maintaining the core- and divertor-plasma parameters established with NBI alone.

Recapitulating, a new NBI-heated confinement regime has been established which develops beyond a critical density and can be maintained for at least 50 energy confinement times (mostly limited by the NBI availability). Since this IC regime appears related to the ELM-free H mode, without the disastrous side effect of impurity accumulation normally accruing at higher densities, it is tentatively being assigned the acronym "high density H-mode" (HDH). The HDH mode exists under a wide variety of magnetic field configurations (separatrix- and limiter-bounded), power levels (1–3.5 MW, corresponding to absorbed power densities of $\simeq$1.2–4 MW/m^3 averaged over the plasma volume), and magnetic fields (0.9–2.5 T). The density profiles are flat, with a steep gradient near the plasma edge, and show high separatrix densities (important for detachment). Energy confinement is in excess of τ_E^{ISS95} over the entire $\bar{n}_e$ range. Impurity confinement is poor, related to reduction of the inwards pinch velocity (a prominent effect in NC discharges), with τ_{imp} approaching τ_E at the highest densities. The impurity radiation profiles are hollow, with edge radiation levels up to 50% of P_{abs} yielding little degradation of τ_E, and up to 90% with acceptable deleterious effects on τ_E. An important aspect of this confinement regime is its quiescent quasistationary state even close to operational boundaries, i.e., $P_{\mathrm{rad}}/P_{\mathrm{abs}}$ up to 90% or $\langle\beta\rangle$ to 3.1%.

In terms of relevance to larger fusion devices, the core plasma is, on one hand, in a marginally collisionless regime, i.e., ν^* is less than one ($\nu^* \simeq 0.2$, at $T_i = 400$ eV, $n_e = 2 \times 10^{20}$ m^{-3} with ν^* = ratio of the ion-ion collision frequency ν^{ii} to the banana bounce frequency $\nu_b \sim \iota_a v_T/R$), but ν^* will be at least a factor of 10 lower on future devices at similar densities. On the other hand, edge fueling always occurs locally under collisional plasma conditions. In any case, our results—successful operation of an island divertor in combination with the discovery of the HDH regime—render excellent prospects for W7-X, the successor experiment of W7-AS.

*Email address: Kent.McCormick@ipp.mpg.de

[1] ITER Divertor Groups, D. E. Post *et al.,* Nucl. Fusion **39**, 2391 (1999).
[2] H. Renner, Nucl. Fusion **40**, 1083 (2000).
[3] U. Stroth *et al.,* Nucl. Fusion **36**, 1063 (1996).
[4] P. Grigull *et al.,* Plasma Phys. Controlled Fusion **43**, A175 (2001).
[5] K. McCormick *et al.,* Plasma Phys. Controlled Fusion **41**, B285 (1999).
[6] K. McCormick *et al.,* J. Nucl. Mater. **290–293**, 920 (2001).
[7] R. Burhenn *et al.,* Europhys. Conf. Abstr. **19c**, 145 (1995); **21a**, 1609 (1997).
[8] L. Giannone *et al.,* Plasma Phys. Controlled Fusion **42**, 603 (2000).
[9] P. Grigull *et al.,* J. Nucl. Mater. **290–293**, 1009 (2001).
[10] R. Burhenn *et al.,* Europhys. Conf. Abstr. **24b**, 1000 (2000).
[11] J. E. Rice *et al.,* Phys. Plasmas **4**, 1605 (1997).
[12] J. P. T. Koponen *et al.,* Nucl. Fusion **40**, 365 (2000).
[13] Y. Feng *et al.,* J. Nucl. Mater. **266–269**, 812 (1999).
[14] Y. Feng *et al.,* Plasma Phys. Controlled Fusion **44**, 611 (2002).
[15] A. Weller *et al.,* Phys. Plasmas **8**, 931 (2001).
[16] M. Greenwald *et al.,* Phys. Plasmas **6**, 1943 (1999); M. Greenwald *et al.,* Plasma Phys. Controlled Fusion **42A**, 263 (2000); J. A. Snipes *et al., ibid.* **43**, L23 (2001).
[17] H. P. Laqua *et al.,* Phys. Rev. Lett. **78**, 3467 (1997).